A Theoretical Investigation of the Methylation of Alkenes with Methanol over Acidic Zeolites

Stian Svelle,[†] Bjørnar Arstad,[†] Stein Kolboe,*[,†] and Ole Swang[‡]

Department of Chemistry, University of Oslo, P.O. Box 1033 Blindern, N-0315 Oslo, Norway, and Department of Hydrocarbon Process Chemistry, SINTEF Applied Chemistry, P.O. Box 124 Blindern, N-0134 Oslo, Norway

Received: October 8, 2002

A quantum chemical investigation of the methylation of alkenes by methanol over acidic zeolite catalysts has been performed. A cluster model consisting of four tetrahedrally coordinated atoms (T-atoms) has been used to represent the zeolite. The activation barrier for methylation is dependent on the size and substitution pattern of the alkene reactant. The results can be rationalized by considering the relative energies of the carbocations that describe the reaction path. Implications for methanol-to-hydrocarbon chemistry are discussed. The effect of zeolite acidity on the activation barrier has also been probed. The barrier decreases when the catalyst acidity is increased.

1. Introduction

Since the discovery of zeolite-catalyzed conversion of methanol to hydrocarbons (MTH), a great research effort has been made to resolve mechanistic issues.[1,2] Initially, focus was directed at the formation of initial C−C bonds and whether ethene or propene was the initial alkene formed. This reaction step has, however, been claimed to be of little interest,[3−5] or even insignificant,[6] because it is clear that, once hydrocarbons are formed, a completely different mechanistic scheme is valid.

During the first years of research, a scheme was proposed where initially formed lower alkenes are methylated to form higher homologues, which, in turn, are cracked into mainly C_2−C_4 alkenes. These either desorb as products or are methylated again. Aromatics were considered to be end products of cyclization and dehydrogenation steps and believed to be coke precursors.[3,5,7,8]

A second, more recent scheme, which is termed the "hydrocarbon pool" mechanism,[9−11] also exists. Initially, a mechanistic cycle that is based on continuous alkylations of unspecified, hydrogen-poor adsorbed species, which could, in turn, split off low alkenes, was suggested. Experiments where benzene or toluene and ^{13}C-methanol were co-reacted have been performed, and it was clear that ethene, propene, and the arenes in the effluent had indistinguishable isotopic distributions.[12] This strongly indicated that methanol conversion could proceed via repeated methylations and dealkylations of aromatic reaction centers. Several later studies have confirmed and clarified this hypothesis, and it seems that methylbenzenes, methylnaphthalenes, and certain methylated cyclic carbenium ions can constitute the hydrocarbon pool.[13−20] There may also be a facile interconversion of these hydrocarbon pool species.

Very recently, theoretical work that is relevant to the MTH reaction mechanism has been published. Activation energies for important reaction steps have been investigated using density functional theory (DFT) and a fairly small cluster (4 tetragonally coordinated atoms (T-atoms), 19 atoms total) as a model catalyst. Vos et al.[21,22] considered the methylation of benzene and toluene to form the next-higher homologue. We have previously analyzed the reactivity of toluene, 1,2,4,5-tetramethylbenzene, and hexamethylbenzene using quantum chemistry.[23] The results indicated that any methylbenzene inside a zeolite pore in the presence of methanol will be completely methylated to form the heptamethylbenzenium ion (if sufficient space is available), because the methylation activation barrier decreases as the number of methyl groups increases. To our best knowledge, no theoretical work on the methylation of alkenes by methanol over zeolites exists in the literature, nor does there seem to be any proper compilation of experimental kinetic data available for these reactions.

In this work, we have investigated the methylation of seven different alkenes, from ethene to 2-methyl-2-butene, using DFT. The aforementioned 19-atom cluster has been used to model the catalyst. The results have direct bearing on MTH chemistry, because it allows an evaluation of parts of the initially proposed mechanistic scheme. Together with previously published results, a direct comparison of the intrinsic reactivity of alkenes versus aromatics is now possible. This information is difficult to obtain experimentally. The findings presented here are also relevant for the formation of aromatic compounds in MTH systems, because this, by necessity, must proceed via the formation of relatively long-chained alkenes. Furthermore, we present an evaluation of the effect of cluster acidity on activation barriers. This important point lies at the very center of acid catalysis research.

2. Computational Details

All calculations were done with the Gaussian98 program package.[24] All geometries were optimized using the B3LYP hybrid density functional and 6-31G* basis sets. No geometric constraints were used. In addition, single-point energies were calculated for these geometries, using the B3LYP/6-311G** and MP2/6-31G* levels of theory. A few single-point energy calculations were also performed using the MP2/6-311G** level of theory. The zeolite catalyst has been modeled using a cluster consisting of four T-atoms, i.e., three Si atoms and one Al atom,

* Author to whom correspondence should be addressed. E-mail: stein.kolboe@kjemi.uio.no.
[†] University of Oslo.
[‡] SINTEF Applied Chemistry.

10.1021/jp022201q CCC: $25.00
Published on Web 08/12/2003

TABLE 1: Products Formed in the Methylation Reactions Investigated

object of methylation	investigated products
ethene	propene, cyclopropane
propene	*trans*-2-butene
1-butene	*trans*-2-pentene
trans-2-butene	2-methyl-2-butene
cis-2-butene	2-methyl-2-butene
isobutene	2-methyl-2-butene
2-methyl-2-butene	2,3-dimethyl-2-butene

to generate the acidic site.[23] This cluster has been used previously to model similar reactions.[21−23] To reduce the effect of using a finite cluster model, care has been taken to ensure that the reactants and products were coordinated to the cluster in a similar manner for all reactions. For all stationary points, vibrational spectra were calculated to ensure that the correct number of imaginary frequencies was at hand, i.e., one imaginary frequency for transition states and zero for energy minima. For the transition states, the normal modes corresponding to the imaginary frequencies were visualized, to confirm that they indeed corresponded to the expected motion of atoms. Intrinsic reaction coordinate (IRC) calculations were, in some cases, performed to investigate the minima connected by the transition states. The transition states were also investigated by perturbing the geometries very slightly along the reaction coordinate, corresponding to the negative eigenvalue in the Hessian, and using the geometries thus produced as starting points for energy minimizations. This quasi-IRC approach appeared to be a more robust procedure than the IRC functionality in Gaussian98 and gave qualitatively identical results as IRC calculations, but at considerably smaller computational cost.

3. Results and Discussion

The methylation of ethene, propene, 1-butene, *trans*-2-butene, *cis*-2-butene, isobutene, and 2-methyl-2-butene has been investigated on a 4 T-atom cluster model. Adsorbed reactants, transition states, protonated products, and final products were optimized as described above. For most of the reactions, the carbenium ion intermediate (see discussion below) could be deprotonated to yield several different product alkenes. In such cases, the thermodynamically most stable alkene was chosen as the product. The products thus selected are listed in Table 1.

The reaction mechanism described here is associative, and it is similar to that reported for the methylation of aromatic compounds.[21−23] Theoretical studies on the methylation of arenes indicate that the associative mechanism is at least as likely as a dissociative pathway, because the first step of the dissociative mechanism (i.e., methoxide formation) was found to have a higher activation energy than single-step, associative methylation.[22] This result also applies to alkene methylation. Also, experimental results favor the associative mechanism for this related reaction.[25] We have not investigated the dissociative pathway.

Figure 1 shows the stationary points on the reaction pathway for the methylation of *trans*-2-butene and is representative of the other reactions. Table 2 lists the energies of the stationary points for all reactions considered, calculated gas-phase reaction energies, and calculated reaction enthalpies. Experimental reaction enthalpies are included for comparison. When energies are discussed, we refer to the B3LYP/6-31G* + ZPE values, unless otherwise stated. Important geometric parameters are listed in Table 3. The atom labels are defined in Figures 2 and 3.

3.1. Reactants and Adsorption Energies. The starting point for all reactions is methanol and an alkene coadsorbed onto the cluster. Methanol is adsorbed end-on onto the acidic site, forming two hydrogen bonds. This is the same adsorption mode as described earlier by several workers.[21,22,27−29] The methyl group of methanol does not point directly toward the alkene double bond; rather, the alkene is located next to the methanol molecule. Different reactant positions, with respect to alkene methyl groups and also the relative positioning of the two reactants, were investigated. All energy differences among the stationary points thus found were very small, i.e., <2 kJ/mol. The reactant geometries were chosen to be as qualitatively similar as possible. Upon coadsorption of methanol and an alkene on the cluster, the $O_{z1}H_z$ distance is considerably stretched, from 0.974 Å to 1.03 Å. The acidic proton is located at a distance of 1.54−1.55 Å from the methanol O atom, and the $O_{z2}H_{m4}$ distance is 1.83 Å. These values are essentially identical to those reported for the coadsorption of methanol and arenes, using the B3LYP functional,[22,23] and are slightly longer (∼0.05 Å) than the values calculated using the MPWPW91 functional.[21]

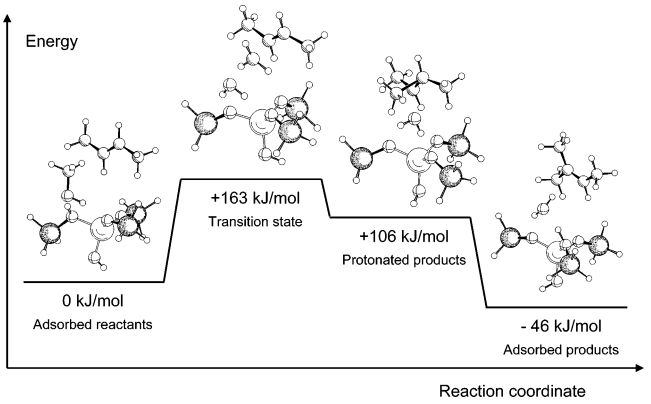

Figure 1. Stationary points on the reaction path for the methylation of *trans*-2-butene.

The coadsorption energies (the first column in Table 2) are essentially the same for all alkenes investigated. The absolute values are 5−15 kJ/mol smaller than those previously reported for the coadsorption of methanol and methylarenes.[23] The calculated adsorption energy is larger when the zero-point energy is excluded (the B3LYP/6-31G* electronic energy). Such a difference can be attributed to the very different vibrational modes of the separated, gas-phase reactants and the reactants in the coadsorbed state. There is, furthermore, a substantial increase in the calculated adsorption energy when ab initio MP2 methodology (MP2/6-31G*//B3LYP/6-31G*) is used rather than DFT. This is expected, because it is well-known that DFT is ill-suited for accurate descriptions of long-range van der Waals interactions.[30,31] There is a decrease in adsorption energy (∼10 kJ/mol) when going from the B3LYP/6-31G* level of theory (without ZPE correction) to the B3LYP/6-311G**// B3LYP/6-31G* level of theory. An increase in the basis set size used in the MP2 single-point energy calculations, from 6-31G* to 6-311G**, has little effect on the adsorption energies.

3.2. Transition States. In the transition state, methanol is protonated and the O−C bond of methanol is significantly stretched. A formal methyl cation leaves the methanol and moves toward the alkene double bond. This CH_3^+ group is almost planar; the H atoms have just moved past the inversion point. The degree of inversion is indicated by the $H_{m1}H_{m2}H_{m3}C_m$ dihedral angles in Table 3. The methyl cation is, in every case, only slightly above the plane defined by O_m and the alkene double bond. This is clear from the $O_mC_{less}C_{more}C_m$ dihedral angles. The imaginary frequencies of the transition states are

TABLE 2: Energies of the Stationary Points for Methylation Reactions and Gas-Phase Reaction Energies[a]

object of methylation	energy (kJ/mol) gas-phase reactants	transition state	protonated alkene	adsorbed products	gas-phase products	gas-phase reaction energy	gas-phase reaction enthalpy (kJ/mol) calculated	experiment[b]
				B3LYP/6-31G* + ZPE				
ethene[c]	87	183	N/A[d]	−56	45	−42	−41	−73
ethene[e]				−11	82	−6	−6	−40
propene	88	169	114	−53	46	−42	−39	−72
1-butene	88	168	112	−53	46	−42	−39	−72
trans-2-butene	88	162	106	−46	53	−34	−32	−75
cis-2-butene	87	161	117	−53	47	−41	−38	−73
isobutene	88	156	N/A[d]	−45	55	−34	−31	−65
2-methyl-2-butene	87	154	97	−40	61	−26	−23	−70
				B3LYP/6-31G*				
ethene[c]	98	184	N/A[d]	−56	60	−38		
ethene[e]				−16	92	−6		
propene	98	170	115	−53	70	−36		
1-butene	99	170	114	−53	62	−37		
trans-2-butene	98	164	108	−46	68	−29		
cis-2-butene	98	164	120	−51	63	−35		
isobutene	99	159	N/A[d]	−44	70	−28		
2-methyl-2-butene	97	156	100	−39	77	−20		
				B3LYP/6-311G**//B3LYP/6-31G*				
ethene[c]	89	184	N/A[d]	−68	36	−53		
ethene[e]				−26	73	−16		
propene	88	171	114	−67	38	−50		
1-butene	88	171	114	−65	39	−49		
trans-2-butene	88	165	104	−58	45	−43		
cis-2-butene	89	163	116	−63	41	−48		
isobutene	88	158	N/A[d]	−57	46	−42		
2-methyl-2-butene	88	155	95	−53	54	−34		
				MP2/6-31G*//B3LYP/6-31G*				
ethene[c]	111 (105)[f]	184 (186)	N/A[d]	−65 (−77)	55 (35)	−56 (−70)		
ethene[e]				−43	73	−38		
propene	114	172	95	−63	59	−55		
1-butene	112	168	90	−70	56	−56		
trans-2-butene	117	162	83	−62	65	−52		
cis-2-butene	109	157	81	−76	51	−58		
isobutene	116	164	N/A[d]	−59	68	−48		
2-methyl-2-butene	110 (106)	147 (148)	73 (72)	−65 (−82)	66 (46)	−44 (−60)		

[a] All values relative to the adsorbed reactants. Enthalpies calculated at 298 K. [b] Experimental reaction enthalpies (298 K) from ref 26. [c] Product formed is propene. [d] All attempts to optimize these structures failed. [e] Product formed is cyclopropane. Gas-phase reactants, adsorbed reactants, and transition state are the same as when propene is the product formed. [f] Numbers in parentheses have been calculated at the MP2/6-311G**//B3LYP/6-31G* level of theory.

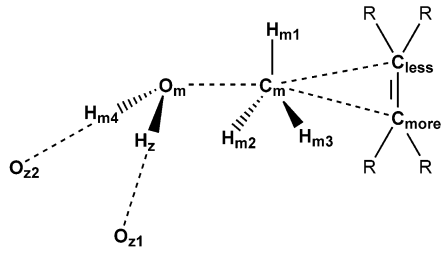

Figure 2. Schematic representation of the transition state for methylation of alkenes. Same atom labels apply for the adsorbed reactants. C_{less} is the less-substituted carbon atom, whereas C_{more} is the more-substituted carbon atom.

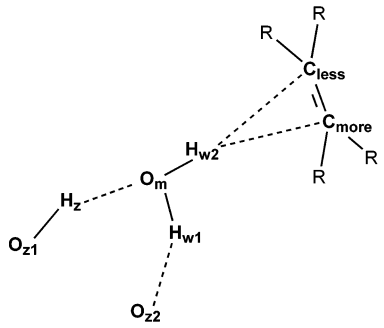

Figure 3. Schematic representation of the adsorbed products. C_{less} is the less-substituted carbon atom, whereas C_{more} is the more-substituted carbon atom.

in the same range as those reported for similar studies on the methylation of arenes,[22] i.e., $\sim 350i$ cm^{-1}.

The manner in which the methyl cation is coordinated to the alkene double bond in the transition state is of considerable interest. For the methylation of ethene, there is a very nearly symmetrical arrangement, and the C_mC_{less} and C_mC_{more} distances are identical ($\Delta R = 0.003$ Å; see Figure 2 for atom label definitions). This indicates that a protonated cyclopropane species is being formed, rather than a primary propyl cation, which is the expected intermediate if the methyl cation is attached to only one of the ethene C atoms. Efforts were made to find a substantially unsymmetrical transition state; however, these efforts either failed or resulted in a shift of geometry toward the nearly symmetrical arrangement presented above. The transition state was then investigated further by performing IRC calculations and employing the previously outlined quasi-IRC procedure. These calculations did indeed proceed via geometries that were very similar to that of protonated cyclopropane. However, no stationary point with such a geometry was found, and the adsorbate resembling protonated cyclopro-

TABLE 3: Geometric Parameters (Distances, Angles, and Dihedral Angles)

	$C_2^=$[a]	$C_2^=$[b]	$C_3^=$	1-$C_4^=$	*t*-2-$C_4^=$	*c*-2-$C_4^=$	*i*-$C_4^=$	$C_5^=$
				Reactants[c]				
distance (Å)								
$O_{z1}H_z$	1.03	[d]	1.03	1.03	1.03	1.03	1.03	1.03
$O_{z2}H_{m4}$	1.83		1.83	1.83	1.83	1.83	1.83	1.83
H_zO_m	1.54		1.54	1.55	1.54	1.55	1.54	1.55
$H_{m4}O_m$	0.99		0.99	0.99	0.99	0.99	0.99	0.99
O_mC_m	1.44		1.44	1.43	1.44	1.43	1.44	1.43
C_mC_{less}	4.06		3.94	4.11	3.93	4.10	3.91	4.07
C_mC_{more}	4.18		4.20	4.14	4.10	4.12	4.23	4.10
$C_{less}C_{more}$	1.33		1.34	1.34	1.34	1.34	1.34	1.34
C_mAl	4.42		4.43	4.38	4.44	4.34	4.42	4.39
angle (deg)								
$H_{m1}H_{m2}H_{m3}C_m$	35.7		35.8	35.9	35.8	35.9	16.7	35.9
$O_mC_{less}C_{more}C_m$	15.7		16.2	13.5	15.8	12.8	35.8	8.9
				Transition States[c]				
distance (Å)								
$O_{z1}H_z$	1.88	[d]	1.85	1.85	1.86	1.81	1.82	1.84
$O_{z2}H_{m4}$	1.93		1.92	1.91	1.89	1.97	1.88	1.87
H_zO_m	0.99		0.99	0.99	0.99	0.99	0.99	0.99
$H_{m4}O_m$	0.98		0.98	0.98	0.99	0.98	0.99	0.99
O_mC_m	2.27		2.23	2.23	2.21	2.21	2.17	2.17
C_mC_{less}	2.14		2.07	2.07	2.19	2.21	2.08	2.14
C_mC_{more}	2.14		2.35	2.35	2.23	2.22	2.50	2.38
$C_{less}C_{more}$	1.36		1.36	1.37	1.37	1.37	1.37	1.37
C_mAl	3.50		3.49	3.50	3.50	3.50	3.52	3.51
angle (deg)								
$H_{m1}H_{m2}H_{m3}C_m$	−14.8		−12.9	−12.7	−11.6	11.3	−10.1	−10.0
$O_mC_{less}C_{more}C_m$	2.2		3.0	3.0	2.2	0.9	2.3	1.7
				Products[e]				
distance (Å)								
$O_{z1}H_z$	1.04	1.03	1.04	1.04	1.04	[f]	[f]	1.04
$O_{z2}H_{w4}$	1.85	1.87	1.88	1.89	1.89			1.88
H_zO_m	1.53	1.55	1.53	1.53	1.53			1.52
$H_{w1}O_m$	0.99	0.99	0.99	0.99	0.99			0.99
$H_{w2}C_w$	0.98	0.98	0.98	0.98	0.98			0.98
$H_{w2}C_{less}$	2.33	2.34	2.29	2.41[g]	2.27			2.32
$H_{w2}C_{more}$	2.47	2.34	2.36	2.33[h]	2.43			2.24
$C_{less}C_{more}$	1.34	1.53[i]	1.34	1.34	1.35			1.36
angle (deg)								
$O_mC_{more}C_{less}H_{w2}$	1.1	3.7	0.2	4.3	3.6			0.2

[a] Product formed is propene. [b] Product formed is cyclopropane. [c] Atom labels are defined in Figure 2. [d] The starting point and transition state are the same as those for the formation of propene. [e] Atom labels are defined in Figure 3. [f] The same product (2-methyl-2-butene) is formed as that for the methylation of *trans*-2-butene. [g] Distance to the methyl-substituted C atom of the double bond. [h] Distance to the ethyl-substituted C atom of the double bond. [i] C−C single bond in cyclopropane.

pane was immediately deprotonated to form cyclopropane. Cyclopropane is not observed as a product under regular MTH conditions,[1] nor is it formed when the methylation of ethene is studied experimentally at extreme feed rates.[32] It must, therefore, be concluded that primarily formed protonated cyclopropane isomerizes into an open-chained propyl cation before deprotonation can occur. Koch et al.[33,34] published a full description of all protonated propene isomers, using the MP2/6-311G** level of theory for geometry optimizations. They concluded that no primary propyl cation exists as an energy minimum, and that the only stable species are the corner-protonated cyclopropane cation and the secondary propyl cation. Furthermore, they found that corner-protonated cyclopropane isomerizes to the secondary cation in a single-step reaction. From the data reported by Koch et al., we have calculated that the barrier is 55.6 kJ/mol (MP4(FC)/6-311G**//MP2/6-311G** + ZPE correction). The geometry optimizations were redone by us, using B3LYP/6-31G* methodology. No primary propyl cation could be optimized as an energy minimum at our level of theory either, and the isomerization barrier was now 41.0 kJ/mol (B3LYP/6-31G* + ZPE correction). This is a small activation energy, compared to that of the first reaction step, and, with a typical preexponential of $10^{12}-10^{13}$ s^{-1}, this corresponds to a rate constant for the isomerization of 10^8-10^9 s^{-1} at 600 K. The predicted ring opening should thus occur readily under normal reaction conditions.

For the other reactions considered, direct formation of secondary carbenium ions (methylation of propene, 1-butene, *trans*-2-butene, and *cis*-2-butene) or tertiary carbenium ions (methylation of isobutene and 2-methyl-2-butene) is possible without hydrogen shifts. The reactions are therefore considerably less complicated, and a description of the reaction path is quite straightforward. A bond is formed between the methyl cation and the less-substituted C atom of the double bond. This is indicated by the C_mC_{less} and C_mC_{more} distances listed in Table 3. The main charge is then located on the more-substituted C atom, C_{more}. When the alkene double bond is symmetrically substituted with methyl groups, these distances are basically identical, as was the case for ethene. The detailed geometries of the cationic species formed will be discussed in the next section.

The calculated activation barriers for the methylation reactions are listed in the second data column of Table 2. The trend observed can be rationalized on the basis of the expected energies of the carbocations formed. According to the Hammond postulate, the activation energies for similar, endothermic

reactions should mimic those of the products. The methylation of ethene leads to the formation of a very unstable cyclopropane carbonium ion, and the barrier is accordingly high. The methylation of propene leads to the formation of a secondary butyl cation, and the barrier is considerably lower than that for ethene. The small difference in barrier between the methylation of propene and 1-butene can be considered to be an effect of the increased charge-stabilizing effect of an ethyl substituent, relative to a methyl group. The barriers for methylation of *cis*-2-butene and *trans*-2-butene are very similar and lower than that for 1-butene. The similarity is expected, because the reactions both lead to the formation of secondary pentyl cations. The lower barrier, relative to that of 1-butene, can be ascribed to the favorable effects of having substituents on both ends of the double bond. Simple inspection of the Mulliken charges reveals that, in the transition state, and also in the resulting cation, there is considerable charge on both C atoms of the double bond; this observation agrees well with chemical intuition. These charges are best stabilized by having methyl groups on both C atoms. The activation energies for the methylation of isobutene and 2-methyl-2-butene are lower still, because of the formation of tertiary carbenium ions and the increased stabilizing effect of the larger alkyl substituents. This line of reasoning is strongly supported by the calculated energies of the adsorbed cations (third data column in Table 2), which follow the activation energies. Note that the cation formed after the methylation of *cis*-2-butene is coordinated to the cluster in a manner that is different from the coordination of the other cations, and the calculated energy is therefore not directly comparable to that of the others.

The geometries of the transition states are also in reasonable agreement with the Hammond postulate, because a lower barrier implies a geometry that is more similar to that at the starting point. The average distance from the methyl cation to the alkene double bond increases, and the distances from the methanol O atom to the methyl cation tend to decrease as the barrier height decreases, although these trends are not perfect. The variations in the degree of inversion of the methyl cation also support this idea.

The order of the activation energies is the same for all levels of theory employed, except for the increase for isobutene that is found when using MP2/6-31G*//B3LYP/6-31G* methodology. In this case, the barrier for the methylation of isobutene is shifted above that for methylation of *cis*- and *trans*-2-butene. However, this does not mean that the rationalization discussed above, which is based on carbenium ion stability, is incorrect. It is important to bear in mind that the activation barriers presented in Table 2 are calculated as the difference between the energy of the coadsorbed reactants and the energies of the transition states. In the case of the four butenes, the stoichiometries are the same and a comparison of the absolute energies is possible. This analysis reveals that the absolute energy of the transition state for the methylation of isobutene is lower than that for the other three butenes at every level of theory, but it also reveals that the starting point lies lower still, when the MP2/6-31G*//B3LYP/6-31G* scheme is used, so that the barrier becomes greater. However, it is not possible to arrive at a decisive conclusion regarding the relative reactivities of the butene isomers, although the bulk of the results suggest that the reactivity is greatest for isobutene.

3.3. Protonated Products. The immediate methylation products are carbenium ions and water, as outlined in the preceding section. These species were optimized as energy minima (except for the methylation of ethene and isobutene, where the optimizations failed). This was confirmed by the vibrational spectra. The cation formed via the transition state for the methylation of propene is shown in detail in Figure 4. Table 4 lists selected geometric parameters. The atom labels are defined in Figure 5. An extensive description of all the cationic species is given as Supporting Information. Whether cations in zeolites are transition states or energy minima in quantum chemistry calculations is a matter of some debate.[35−43] Kazansky and co-workers[37−43] have shown that the chemisorption of alkenes proceeds via transition states that closely resemble carbenium ions and have concluded that free carbenium ions do not exist as energy minima when an alkene is coordinated to cluster models (in the absence of water). Vos and co-workers[21,22] investigated the methylation of arenes along the very same reaction mechanism as that in this work and did not report any charged intermediates within the cluster approach. However, Arstad et al.[23] very recently published contradictive results, where coadsorbed water and protonated arenes were found to be energy minima, using the same cluster as Vos et al. In that case,[23] removal of the water molecule resulted in the formation of a C−O bond between the hydrocarbon and the cluster.

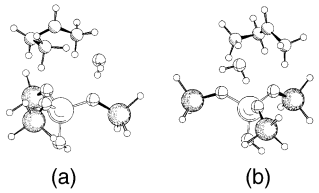

Figure 4. (a) Front and (b) side view (90°) of the adsorbed cation formed after the methylation of propene.

All cations are stabilized through hydrogen bonds with the cluster and the water molecule. These stabilizing interactions are indicated by the fairly short H_2O_m and H_1O_{z1} distances. The C_1H_1 and C_1H_2 bonds are correspondingly stretched. Because of these very favorable interactions between the cations and the cluster, water is partially displaced and only one hydrogen bond between water and the cluster is formed. The other water hydrogen is pointing away from the cluster. This is an effect of the limited cluster size and may be considered to be a cluster artifact. In a real zeolite catalyst, there would be several zeolitic O atoms available for the formation of hydrogen bonds. The presence of water seems to be crucial for the existence of cationic species as energy minima in at least two ways. First, the water molecule functions as a wedge, thus separating the cation and the cluster and preventing deprotonation. Second, the strong interaction between one water H molecule and one zeolite O atom effectively reduces the proton affinity of the cluster, thereby also reducing the probability of deprotonation. Jeanvoine et al.[44] found a similar effect when using molecular dynamics (MD) to study water in chabazite. They found that the presence of a second water molecule was required to facilitate water protonation and hydroxonium ion formation. Termath et al.[45] and Štich et al.[46] also found that increasing the loading of molecules enhances the probability of protonation when employing MD to study water and methanol in zeolites, respectively.

Formally, the positive charge is located on C_3 (Figure 5), and the substituents on this atom are arranged in a very nearly planar, trigonal fashion; thus, the $C_2R_2R_1C_3$ dihedral angle, in every case, is almost zero. The butyl and pentyl cations described in Table 4 have sharp $C_1C_2C_3$ angles and short C_1C_3 distances, which are only slightly longer than the C_1C_2 distance. The C_2C_3 distance is only ∼0.1 Å longer than the distance of

TABLE 4: Geometric Parameters (Distances, Angles, and Dihedral Angles) for Adsorbed Cationic Species

	$C_2^=$	$C_3^=$	1-$C_4^=$	*t*-2-$C_4^=$	*c*-2-$C_4^=$	*i*-$C_4^=$	$C_5^=$
				Protonated Products[a]			
R_1	N/A[b]	−H	−H	$-CH_3$	$-CH_3$	N/A[b]	$-CH_3$
R_2		$-CH_3$	$-CH_2CH_3$	−H	−H		$-CH_3$
R_3		−H	−H	−H	$-CH_3$		$-CH_3$
R_4[c]		−H	−H	$-CH_3$	−H		−H
distance (Å)							
H_1O_{z1}		1.92	1.91	1.89	1.95		2.06
H_2O_m		1.86	1.87	1.87	[d]		2.03
C_1H_1		1.11	1.11	1.12	1.12		1.10
C_1H_2		1.13	1.13	1.12	1.09		1.11
$H_{w1}O_{z2}$		1.73	1.73	1.74	1.83		1.76
C_1C_2		1.64	1.65	1.70	1.67		1.64
C_2C_3		1.41	1.41	1.41	1.41		1.43
C_1C_3		1.83	1.83	1.79	1.84		2.04
angle (deg)							
$C_1C_2C_3$		73.3	73.2	69.5	72.8		83.1
$C_2R_2R_1C_3$		6.4	7.0	7.8	4.3		2.0
distance (Å)							
R_4O_{z1}		3.33	3.26	[e]	4.36		3.48
R_4O_{z3}		2.22	2.20	[e]	3.04		2.23
C_2R_4		1.09	1.09	[e]	1.09		1.09

[a] Atom labels are defined in Figure 5. [b] All attempts to optimize these structures failed. [c] R_4 is, in most cases, the proton that is transferred back to the zeolite to yield the described products. [d] The three H atoms on C_1 are located at distances of 2.66, 2.69, and 2.88 Å from the O_m atom. [e] For the cation formed after the methylation of *trans*-2-butene, there is a different arrangement; the proton that is to be returned points away from the cluster, and a methyl group points down toward the cluster instead.

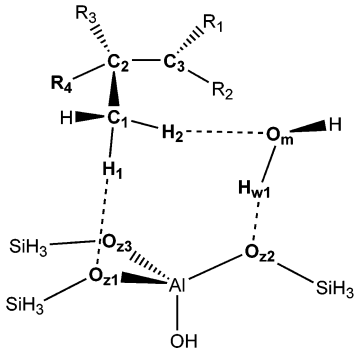

Figure 5. Schematic representation of an adsorbed cation.

the original double bond. It therefore becomes a matter of personal preference whether these species should be considered carbenium ions or methyl-substituted cyclopropane carbonium ions. Sieber et al.[47] used quantum chemistry to give an extensive gas-phase description of $C_4H_9^+$ cations, using MP2(full)/6-31G** for geometry optimizations, and Fărcaşiu and Norton[48] published a similar investigation of the secondary and tertiary pentyl cations, using MP2/6-31G** for optimizations. These authors concluded that the open-chain, secondary C_4 and C_5 cations are transition states rather than energy minima. The secondary cations are always stabilized as more- or less-bridged species. $C_1C_2C_3$ angles of 62.5° and 66.4° are reported for gas-phase geometries of cations very similar to those formed after the methylation of *cis*- and *trans*-2-butene, respectively. These angles are even sharper than those listed in Table 4. The C_2C_3 distances produced by these high-level calculations are in the range 1.397−1.403 Å, which is slightly shorter than the distances presented in this work. The geometries presented for the energy minima in refs 47 and 48 are thus in good agreement with the results presented here.

The adsorption mode of the cation formed after the methylation of *cis*-2-butene is different from that of the others. The C_1 methyl group is rotated and there is no proper interaction between any of the hydrogen atoms on C_1 and the water molecule; the shortest distance is 2.66 Å. The energy is therefore higher than that of any of the other cationic species. However, the energy is substantially lowered at the MP2/6-31G*//B3LYP/6-31G* level of theory. This may be explained by the superior description of long-range interactions inherent in this method.

The hexyl cation formed after the methylation of 2-methyl-2-butene is less bridged than the other ions. The C_1C_3 distance is longer and the $C_1C_2C_3$ angle is less sharp. This is probably because the formal charge on C_3, which, in this case, is a tertiary C atom, is fairly well stabilized. Hence, the tendency for formation of a bridged species is reduced. It is noteworthy that this cation, at the MP2/6-31G*//B3LYP/6-31G* level of theory, lies only 73 kJ/mol above the adsorbed reactants.

The R_4O_{z3} distances listed in Table 4 are, for several species, quite short (R_4 is, in most cases, the proton that is transferred back to the zeolite to yield the described products). Even though this proton points directly toward a zeolite O atom, spontaneous deprotonation does not occur. The geometry around C_2 partially explains this observation. During deprotonation, C_2 will gradually adopt sp^2 geometry. This represents considerable distortions; both the H_1O_{z1} and H_2O_m interactions will be at least partially weakened. This seems to be the main reason these structures are energy minima.

The failure to optimize the protonated cyclopropane carbonium ion and water on the cluster was not surprising. This molecule is the smallest of the series, and it, therefore, has the greatest mobility on the cluster. It is, thus, more prone to deprotonation. Also, it is considerably less stable energetically than the other species investigated. It was, however, less obvious that all attempts to optimize the cation formed after the methylation of isobutene should fail. The potential energy surface (PES) is extremely flat around a geometry that corresponds to the hypothesized cation (see Figure S6 of the Supporting Information). No energy minimum could be found, however, even though two of four convergence criteria were fulfilled at one point. The electronic energy was then 99 kJ/mol greater than that of the adsorbed reactants, which fits well with the main trend in Table 2. The geometry was similar to that of the cations reported for the other methylations, i.e., a bridged species. It is not possible to exclude the existence of a shallow energy minimum; however, it may be that, in this

particular case, the cation is an inflection point on the PES, rather than a minimum.

The deprotonation of the butyl cation formed after the methylation of propene was investigated more thoroughly, and an activation energy for proton loss of 6 kJ/mol (8 kJ/mol without ZPE correction) was found. An identical value (6 kJ/mol) was found at the B3LYP/6-311G**//B3LYP/6-31G* level of theory, and the barrier was 23 kJ/mol when using MP2/6-31G*//B3LYP/6-31G* methodology. The deprotonation transition state describes a slight movement of the methyl group bonded to C_3 toward the water molecule. The quasi-IRC approach was applied and revealed that, in a concerted reaction, one of the protons of the methyl group is transferred to the water molecule and the H_{w1} atom (which is the water proton pointing toward a zeolite O atom) is returned to the cluster. This results in the formation of 1-butene and water. The very low barrier indicates that proton loss will occur instantaneously under experimental conditions. Indeed, there have been no experimental observations of aliphatic carbenium ions in zeolites. The stationary points described previously are, nonetheless, quite descriptive for the reaction pathway of the methylation reactions studied and serve to elaborate the role of carbenium-ion-like species in zeolites.

3.4. Products and Reaction Energies. The final products (water and the deprotonated alkene with one more C atom than the reactant) are also coadsorbed onto the cluster. The water molecule is hydrogen-bonded to the acidic site, and the alkene is associated with the water molecule. The reaction energies for the adsorbed products are more exothermic than the gas-phase energies. This, of course, indicates that the products are more strongly adsorbed than the reactants, by ~15 kJ/mol. As expected, the differences between calculated reaction enthalpies at 298 K and the zero-point corrected reaction energies (both at B3LYP/6-31G*) are very small. Increasing the size of the basis set used in combination with the B3LYP functional causes the reaction energies to move somewhat closer to the experimental values. Going from B3LYP/6-311G**//B3LYP/6-31G* to MP2/6-31G*//B3LYP/6-31G* methodology represents a small improvement, but only at the MP2/6-311G**//B3LYP/6-31G* level of theory is it possible to achieve fair agreement with the experimental values. It seems that this fairly advanced method is required to reproduce the reaction energies of nonisodesmic reactions properly. The small variations in the experimental values are not reproduced by any of the methods.

3.5. Bearings on Methanol-to-Hydrocarbon Chemistry. The results presented above have important relevance to methanol-to-hydrocarbon (MTH) chemistry in several ways. Ethene has a considerably higher barrier for methylation than any of the other alkenes investigated, and a low reactivity is predicted. This has been confirmed by experimental results by Dahl and Kolboe.[9,10] They observed experimentally that ethene shows little reactivity when co-reacted with methanol over SAPO-34, which is a zeolite-like catalyst, and it was concluded that ethene is not likely to have an important role as a reaction intermediate. The next-higher homologue, propene, has a lower barrier, and this trend is upheld when comparing propene with the butenes and the butenes with 2-methyl-2-butene. The MTH reaction is described as autocatalytic, and this is most often observed as a large increase in the initial methanol conversion when any hydrocarbon is added to the methanol feedstock.[4,7,49,50] The results presented here further elucidate this aspect of MTH chemistry, because we have shown that the product from one reaction step (methylation) is more reactive than the initial reactant.

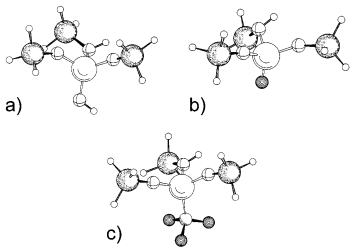

Figure 6. Three cluster models with different terminating groups and acidity ((a) −OH cluster, (b) −F cluster, and (c) $-CF_3$ cluster).

We have previously investigated the reactivity of methyl-substituted arenes with the same methods as those used here. The barriers for methylation of toluene, 1,2,4,5-tetramethylbenzene, and hexamethylbenzene were found to be 187, 171, and 169 kJ/mol (B3LYP/6-31G* + ZPE correction), respectively.[23] This is in the very same range as the barriers presented here, and it must be concluded that arenes and alkenes have very similar activity in methylation reactions. One important factor that has not been considered so far is the pre-exponential. This factor may be somewhat larger for arenes than for alkenes, because an aromatic ring formally has three double bonds, which can all be methylated. This fact means that the arene has several reactive sites, compared to the lone double bond of an alkene.

3.6. Effect of Zeolite Cluster Proton Affinity. The effect of cluster acidity or proton affinity was investigated by constructing two zeolite clusters that are different from the model discussed so far. We substituted the terminal −OH group that is bonded to the Al T-atom with −F and $-CF_3$ groups. The overall compositions of these new models are then $H^+[(F)Al(OSiH_3)_3]^-$ and $H^+[(F_3C)Al(OSiH_3)_3]^-$, as shown in Figure 6. The proton affinity of the regular, −OH-substituted deprotonated cluster is 1256 kJ/mol, and our approach allowed a tuning of the proton affinities over a range of 40 kJ/mol. Zeolite acid strength is claimed to be in the range of strong acids, rather than that of superacids.[35] The HSO_4^- anion has an experimentally determined gas-phase proton affinity of 1282 kJ/mol,[26] which compares well with the acidity of our cluster model. On the other hand, Nicholas and Haw[51] determined that a hydrocarbon with a proton affinity of >874 kJ/mol will be protonated and form a stable carbenium ion within the zeolite pores. This value is considerably lower than a gas-phase proton affinity, because of the electrostatic stabilization of the ion pair. Studies relying on periodical boundary conditions and plane wave basis sets, which include interactions with the entire zeolite framework, have shown that charged species and transition states are stabilized by 20%−50%,[21,52,53] compared to the cluster approach. Although the cluster model is a good qualitative model of an acidic site, it seems reasonable to assume that the model does not fully simulate the quantitative acid strength of a real zeolite catalyst.

The methylation of propene was selected as a probe reaction, and the activation barriers (calculated as before) are displayed in Table 5. Selected geometric parameters for the stationary points are listed in Table 6. It is clear that the activation energy is strongly dependent on the cluster proton affinity. The difference of 40 kJ/mol in proton affinity results in a shift in activation energy of 13 kJ/mol, corresponding to a change by a factor of 14 in the reaction rate at 600 K. This relationship is the same for all methods used, although the absolute value of the cluster proton affinity is sensitive to the calculation methodology. This correlation between catalyst acidity and activation energy is probably strongest when the zeolite proton is completely transferred to the reactants in the transition state,

TABLE 5: Proton Affinities of Three Differently Substituted Zeolite Clusters and Activation Energies for the Methylation of Propene

cluster substituent	cluster proton affinity (kJ/mol)	activation energy (kJ/mol)	reaction energy (kJ/mol)
	B3LYP/6-31G* + ZPE		
−OH	1256	169	−53
−F	1242	161	−55
$-CF_3$	1217	156	−56
	B3LYP/6-31G*		
−OH	1289	170	−53
−F	1274	161	−55
$-CF_3$	1249	156	−56
	B3LYP/6-311G**//B3LYP/6-31G*		
−OH	1295	171	−67
−F	1275	161	−69
$-CF_3$	1251	155	−73
	MP2/6-31G*//B3LYP/6-31G*		
−OH	1284	172	−64
−F	1267	164	−65
$-CF_3$	1239	159	−65

TABLE 6: Geometric Parameters (Distances, Angles, and Dihedral Angles) for the Methylation of Propene with Three Different Cluster Models (−OH, −F, and $-CF_3$)

	−OH	−F	$-CF_3$
	Reactants[a]		
distance (Å)			
$O_{z1}H_z$	1.03	1.04	1.05
$O_{z2}H_{m4}$	1.83	1.83	1.82
H_zO_m	1.54	1.52	1.49
$H_{m4}O_m$	0.99	0.99	0.99
O_mC_m	1.44	1.44	1.44
C_mC_{less}	3.94	3.93	3.93
C_mC_{more}	4.20	4.19	4.19
$C_{less}C_{more}$	1.34	1.34	1.34
C_mAl	4.43	4.40	4.36
angle (deg)			
$H_{m1}H_{m2}H_{m3}C_m$	35.8	35.6	35.6
$O_mC_{less}C_{more}C_m$	16.2	16.5	16.8
	Transition States[a]		
distance (Å)			
$O_{z1}H_z$	1.85	1.88	1.88
$O_{z2}H_{m4}$	1.92	1.89	1.92
H_zO_m	0.99	0.99	0.99
$H_{m4}O_m$	0.98	0.99	0.98
O_mC_m	2.23	2.22	2.22
C_mC_{less}	2.07	2.08	2.08
C_mC_{more}	2.35	2.36	2.36
$C_{less}C_{more}$	1.36	1.36	1.36
C_mAl	3.49	3.46	3.48
angle (deg)			
$H_{m1}H_{m2}H_{m3}C_m$	−12.9	−12.2	−12.3
$O_mC_{less}C_{more}C_m$	3.0	2.9	3.0
	Products[b]		
distance (Å)			
$O_{z1}H_z$	1.04	1.04	1.05
$O_{z2}H_{w4}$	1.88	1.86	1.85
H_zO_m	1.53	1.51	1.48
$H_{w1}O_m$	0.99	0.99	0.99
$H_{w2}C_w$	0.98	0.98	0.98
$H_{w2}C_{less}$	2.29	2.29	2.29
$H_{w2}C_{more}$	2.36	2.36	2.35
$C_{less}C_{more}$	1.34	1.34	1.34
angle (deg)			
$O_mC_{more}C_{less}H_{w2}$	0.2	0.6	0.3

[a] Atom labels are defined in Figure 2. [b] Atom labels are defined in Figure 3.

which is the case for the selected model reaction. We suspect that, for a reaction involving a lesser degree of proton transfer in the transition state, any such dependence would be reduced.

The increased acid strength is also reflected in the geometries of the stationary points. For the adsorbed reactants, the $O_{z1}H_z$ distance follows the cluster proton acidity nicely. Notably, this distance is the same for all three clusters when no adsorbate is present, i.e., 0.974 Å. The H_zO_m distance is shortened when the proton acidity decreases, indicating the formation of a stronger hydrogen bond between the zeolite and methanol. The same trends are observed for the adsorbed products. These effects are less pronounced for the transition states, where there are no clear variations that can be related to the acid strength.

4. Conclusions

A quantum chemical investigation of the methylation of different alkenes by methanol on a zeolite cluster model has been performed. An associative mechanism has been assumed. The activation barrier decreases as the size of the alkene increases, i.e., the product from one reaction step is more reactive than the initial reactant. The activation barriers are in the same range as those reported for methylation of arenes. Therefore, in regard to methylation by methanol, the results do not indicate a significant difference in activity between the two groups of hydrocarbons.

Charged intermediates have been optimized as shallow energy minima for most of the reactions investigated. These carbocations are always bridged species, similar to the expected structure of protonated cyclopropane derivatives. The geometries are in good agreement with high-level gas-phase calculations that have been reported in the literature. The presence of water is important to stabilize the charged species on the cluster model. A barrier for deprotonation was, in one case, calculated and found to be merely 6 kJ/mol, indicating immediate deprotonation. Although these species will not be persistent under experimental conditions, they describe the reaction path for the studied methylation reactions. The lifetime of these species will be so short that obtaining experimental proof of their existence may be impossible.

The activation barrier for methylation of propene has been found to vary significantly, by 13 kJ/mol, when the cluster proton affinity is tuned over a range of 40 kJ/mol.

Acknowledgment. Thanks are due to the Norwegian Research Council for financial support (through Grant Nos. 135867/431 and 149326/431) and a grant of computer time through the NOTUR project (Account Nos. NN2147K and NN2878K).

Supporting Information Available: Thorough descriptions of the geometries and illustrations of the adsorbed cationic species and a description of the PES around the cation formed after the methylation of isobutene (PDF). This material is available free of charge via the Internet at http://pubs.acs.org.

References and Notes

(1) Stöcker, M. *Microporous Mesoporous Mater.* **1999**, *29*, 3−48.
(2) Chang, C. D. The Methanol-to-Hydrocarbons Reaction: A Mechanistic Perspective. In *Shape Selective Catalysis*; Song, C., Garcés, J. M., Sugi, Y., Eds.; ACS Symposium Series 738; American Chemical Society: Washington, DC, 2000; pp 96−114.
(3) Dessau, R. M.; LaPierre, R. B. *J. Catal.* **1982**, *78*, 136−141.
(4) Kolboe, S. *Acta Chem. Scand., Ser. A* **1986**, *A40*, 711−713.
(5) Dessau, R. M. *J. Catal.* **1986**, *99*, 111−116.
(6) Song, W.; Marcus, D. M.; Fu, H.; Ehresmann, J. O.; Haw, J. F. *J. Am. Chem. Soc.* **2002**, *124*, 3844−3845.
(7) Chen, N. Y.; Reagan, W. J. *J. Catal.* **1979**, *59*, 123−129.
(8) Chang, C. D. *Catal. Rev.—Sci. Eng.* **1983**, *25*, 1−118.
(9) Dahl, I. M.; Kolboe, S. *Catal. Lett.* **1993**, *20*, 329−336.
(10) Dahl, I. M.; Kolboe, S. *J. Catal.* **1994**, *149*, 458−464.

(11) Dahl, I. M.; Kolboe, S. *J. Catal.* **1996**, *161*, 304−309.
(12) Mikkelsen, Ø.; Rønning, P. O.; Kolboe, S. *Microporous Mesoporous Mater.* **2000**, *40*, 95−113.
(13) Arstad, B.; Kolboe, S. *Catal. Lett.* **2001**, *71*, 209−212.
(14) Arstad, B.; Kolboe, S. *J. Am. Chem. Soc.* **2001**, *123*, 8137−8138.
(15) Bjørgen, M.; Olsbye, U.; Kolboe, S. *J. Catal.* **2003**, *215*, 30−44.
(16) Haw, J. F.; Nicholas, J. B.; Song, W.; Deng, F.; Wang, Z.; Xu, T.; Heneghan, C. S. *J. Am. Chem. Soc.* **2000**, *122*, 4763−4775.
(17) Goguen, P. W.; Xu, T.; Barich, D. H.; Skloss, T. W.; Song, W.; Wang, Z.; Nicholas, J. B.; Haw, J. F. *J. Am. Chem. Soc.* **1998**, *120*, 2650−2651.
(18) Sassi, A.; Wildman, M. A.; Ahn, H. J.; Prasad, P.; Nicholas, J. B.; Haw, J. F. *J. Phys. Chem. B* **2002**, *106*, 2294−2303.
(19) Song, W.; Haw, J. F.; Nicholas, J. B.; Heneghan, C. S. *J. Am. Chem. Soc.* **2000**, *122*, 10726−10727.
(20) Song, W.; Fu, H.; Haw, J. F. *J. Phys. Chem. B* **2001**, *105*, 12839−12843.
(21) Vos, A. M.; Rozanska, X.; Schoonheydt, R. A.; van Santen, R. A.; Hutschka, F.; Hafner, J. *J. Am. Chem. Soc.* **2001**, *123*, 2799−2809.
(22) Vos, A. M.; Nulens, K. H. L.; De Proft, F.; Schoonheydt, R. A.; Geerlings, P. *J. Phys. Chem. B* **2002**, *106*, 2026−2034.
(23) Arstad, B.; Swang, O.; Kolboe, S. *J. Phys. Chem. B* **2002**, *106*, 12722−12726.
(24) Frisch, M. J.; Trucks, G. W.; Schlegel, H. B.; Scuseria, G. E.; Robb, M. A.; Cheeseman, J. R.; Zakrzewski, V. G.; Montgomery, J. A., Jr.; Stratmann, R. E.; Burant, J. C.; Dapprich, S.; Millam, J. M.; Daniels, A. D.; Kudin, K. N.; Strain, M. C.; Farkas, O.; Tomasi, J.; Barone, V.; Cossi, M.; Cammi, R.; Mennucci, B.; Pomelli, C.; Adamo, C.; Clifford, S.; Ochterski, J.; Petersson, G. A.; Ayala, P. Y.; Cui, Q.; Morokuma, K.; Malick, D. K.; Rabuck, A. D.; Raghavachari, K.; Foresman, J. B.; Cioslowski, J.; Ortiz, J. V.; Stefanov, B. B.; Liu, G.; Liashenko, A.; Piskorz, P.; Komaromi, I.; Gomperts, R.; Martin, R. L.; Fox, D. J.; Keith, T.; Al-Laham, M. A.; Peng, C. Y.; Nanayakkara, A.; Gonzalez, C.; Challacombe, M.; Gill, P. M. W.; Johnson, B. G.; Chen, W.; Wong, M. W.; Andres, J. L.; Head-Gordon, M.; Replogle, E. S.; Pople, J. A. *Gaussian 98*, revision A.11; Gaussian, Inc.: Pittsburgh, PA, 1998.
(25) Ivanova, I. I.; Corma, A. *J. Phys. Chem. B* **1997**, *101*, 547−551.
(26) Thermodynamic data were taken from the NIST database (http://webbook.nist.gov/chemistry).
(27) Zicovich-Wilson, C. M.; Viruela, P.; Corma, A. *J. Phys. Chem.* **1995**, *99*, 13224−13231.
(28) Blaszkowski, S. R.; van Santen, R. A. *J. Phys. Chem.* **1995**, *99*, 11728−11738.
(29) Blaszkowski, S. R.; van Santen, R. A. *J. Phys. Chem. B* **1997**, *101*, 2292−2305.
(30) Sauer, J.; Ugliengo, P.; Garrone, E.; Saunders, V. R. *Chem. Rev.* **1994**, *94*, 2095−2160.
(31) Kurita, N.; Sekino, H. *Chem. Phys. Lett.* **2001**, *348*, 139−146.
(32) Svelle, S.; Rønning, P. O.; Kolboe, S., in preparation.
(33) Koch, W.; Schleyer, P. v. R.; Buzek, P.; Liu, B. *Croat. Chem. Acta* **1992**, *65*, 655−672.
(34) Koch, W.; Liu, B.; Schleyer, P. v. R. *J. Am. Chem. Soc.* **1989**, *111*, 3479−3480.
(35) Martens, J. A.; Jacobs, P. A. An Introduction to Acid Catalysis with Zeolites in Hydrocarbon Reactions. In *An Introduction to Zeolite Science and Practice*; van Bekkum, H., Flanigen, E. M., Jacobs, P. A., Jansen, J. C., Eds.; Studies in Surface Science and Catalysis 137; Elsevier Science: Amsterdam, 2001; pp 633−672.
(36) Frash, M. V.; van Santen, R. A. *Top. Catal.* **1999**, *9*, 191−205.
(37) Kazansky, V. B.; Senchenya, I. N. *J. Catal.* **1989**, *119*, 108−120.
(38) Kazansky, V. B.; Frash, M. V.; van Santen, R. A. *Appl. Catal. A* **1996**, *146*, 225−247.
(39) Kazansky, V. B.; Frash, M. V.; van Santen, R. A. Quantum-Chemical Study of the Nonclassical Carbonium Ion-Like Transition States in Isobutane Cracking on Zeolites. In *11th International Congress on Catalysis−40th Anniversary, Part B*; Hightower, J. W., Delgass, W. N., Iglesia, E., Bell, A. T., Eds.; Studies in Surface Science and Catalysis 101; Elsevier Science: Amsterdam, 1996; pp 1233−1242.
(40) Frash, M. V.; Solkan, V. N.; Kazansky, V. B. *J. Chem. Soc., Faraday Trans.* **1997**, *93*, 515−520.
(41) Frash, M. V.; Kazansky, V. B.; Rigby, A. M.; van Santen, R. A. *J. Phys. Chem. B* **1997**, *101*, 5346−5351.
(42) Frash, M. V.; Kazansky, V. B.; Rigby, A. M.; van Santen, R. A. *J. Phys. Chem. B* **1998**, *102*, 2232−2238.
(43) Kazansky, V. B. *Catal. Today* **1999**, *51*, 419−434.
(44) Jeanvoine, Y.; Ángyán, J. G.; Kresse, G.; Hafner, J. *J. Phys. Chem. B* **1998**, *102*, 7307−7310.
(45) Termath, V.; Haase, F.; Sauer, J.; Hutter, J.; Parrinello, M. *J. Am. Chem. Soc.* **1998**, *120*, 8512−8516.
(46) Štich, I.; Gale, J. D.; Terakura, K.; Payne, M. C. *J. Am. Chem. Soc.* **1999**, *121*, 3292−3302.
(47) Sieber, S.; Buzek, P.; Schleyer, P. v. R.; Koch, W.; Carneiro, J. W. d. M. *J. Am. Chem. Soc.* **1993**, *115*, 259−270.
(48) Fărcaşiu, D.; Norton, S. H. *J. Org. Chem.* **1997**, *62*, 5374−5379.
(49) Mole, T.; Whiteside, J. A.; Seddon, D. *J. Catal.* **1983**, *82*, 261−266.
(50) Mole, T.; Bett, G.; Seddon, D. *J. Catal.* **1983**, *84*, 435−445.
(51) Nicholas, J. B.; Haw, J. F. *J. Am. Chem. Soc.* **1998**, *120*, 11804−11805.
(52) Rozanska, X.; van Santen, R. A.; Hutschka, F. *J. Phys. Chem. B* **2002**, *106*, 4652−4657.
(53) Sauer, J.; Sierka, M.; Haase, F. Acidic Catalysis by Zeolites: Ab Initio Modeling of Transition States. In *Transition State Modeling for Catalysis*; Truhlar, D. G., Morokuma, K., Eds.; ACS Symposium Series 721; American Chemical Society: Washington, DC, 1999; pp 358−367.